Overstraining of flush plain cross-bored cylinders

J M Kihiu, G O Rading and S M Mutuli

Proceedings of the Institution of Mechanical Engineers, Part C: Journal of Mechanical Engineering Science 2004 218: 143
DOI: 10.1243/095440604322887125

Overstraining of flush plain cross-bored cylinders

J M Kihiu[1*], **G O Rading**[2] and **S M Mutuli**[2]
[1] Department of Mechanical Engineering, Jomo Kenyatta University of Agriculture and Technology, Nairobi, Kenya
[2] Department of Mechanical Engineering, University of Nairobi, Kenya

Abstract: A three-dimensional finite element method computer program was developed to establish the elastic–plastic, residual and service stress distributions in thick-walled cylinders with flush and non-protruding plain cross bores under internal pressure. The displacement formulation and eight-noded brick isoparametric elements were used. The incremental theory of plasticity with a 5 per cent yield condition (an element is assumed to have yielded when the effective stress is within 5 per cent of the material yield stress) and von Mises yield criterion were assumed. The frontal solution technique was used. The incipient yield pressure and the pressure resulting in a 0.3 per cent overstrain ratio were established for various cylinder thickness ratios and cross bore–main bore radius ratios. For a thickness ratio of 2.25 and a cross bore–main bore radius ratio of 0.1, the stresses were determined for varying overstrain and an optimum overstrain ratio of 37 per cent was established. To find the accuracy of the results, the more stringent yield condition of 0.5 per cent was also considered. The benefits of autofrettage were presented and alternative autofrettage and yield condition procedures proposed.

Keywords: flush plain cross-bored cylinders, overstrain ratio, autofrettage, stress

NOTATION

C	material constant
d	cross bore–main bore radius ratio
k	thickness ratio
n	strain hardening exponent
R_i	inner radius
R_o	outer radius
Y_s	yield stress
$\overline{\varepsilon^n}$	effective strain
$\overline{\sigma}$	effective stress

1 INTRODUCTION

In 1698, the pressure vessel was used in the form of a steam boiler for the first time {**1**}. The early boilers operated at around 0.048 MPa. Improvement in materials raised this pressure though the boilers were not redesigned. This resulted in several catastrophic failures {**2**}. Current applications such as isostatic compaction of metallic and ceramic powders involve pressures as high as 300 MPa {**3**}. With pressure vessels holding high potential energy exerted by the working fluid, it is important to minimize or even eliminate accidental losses due to poor designs that may result from inadequate understanding of the stresses.

Pressure vessels are usually constructed with side openings for relief, safety valves, etc. {**4**}, which introduce geometric discontinuities on the body of the pressure vessel. In service, the intersection of the cross bore and the cylinder bore forms a stress singularity curve having high relative stresses and sharp stress gradients {**5**}. These high stresses reduce the pressure-carrying capacity of such vessels below that of a plain cylinder. A proper understanding of the stress severity in these regions of high stress fields would lead to usage of low safety factors, economic use of materials, enhanced operating life, lower operating costs and a reduction in losses due to catastrophic or disruptive failures.

For high-pressure applications, a true representation of the state of stress in the presence of side bores is needed because fatigue life is critical and limitations of strength and ductility prevent high factors of safety {**6**}. In design, the ASME Boiler and Pressure Vessel Code does not enforce a detailed stress analysis but only sets the wall thickness necessary to keep the basic hoop stress below an allowable stress. The higher localized

The MS was received on 2 July 2003 and was accepted after revision for publication on 17 November 2003.
* *Corresponding author: Department of Mechanical Engineering, Jomo Kenyatta University of Agriculture and Technology, PO Box 62000, Nairobi, Kenya.*

stresses are taken care of by the safety factor and a set of design rules {**7**}, assuming that any localized yielding in ductile materials results in stress redistributions.

Though this code provides a quick design procedure, it is certainly inadequate for pressure vessels with cross bores, especially when autofrettaged. Pressure vessels are normally subjected to pressures of 1.25–1.5 times the limit pressure at the end of the fabrication process {**8**}. This applied pressure causes yielding of the most highly stressed parts of the structure. After the release of the pressure, residual stresses are left in the structure. For cylinders with cross bores it is important to establish the exact relationship between the overstrain pressure (OVP) and the residual and service stresses. The nature of the resultant stress distributions is also important. The OVP is the internal pressure that results in a desired value of overstrain ratio (OVR) in the cylinder. The OVR is the ratio of the elastic–plastic interface radial distance, referenced at the main bore, to the wall thickness, expressed as a percentage. Overstrain is the process of inducing a desired OVR in a cylinder by application of internal pressure.

Cylinders carrying fluids at high pressures are now of great importance in many industries and their economic use often depends upon the occurrence of small controlled permanent deformations {**9**}. In some cases, autofrettage is done during manufacture when a pressure greater than the leak test pressure is applied. This process results in higher residual stresses and a stronger cylinder, with service stresses being more uniformly distributed across the thickness. In the presence of cross bores, this distribution is not obvious and detailed analysis is necessary.

2 LITERATURE SURVEY

Bursting pressure and overstrain experimental studies to determine the pressure-carrying capacity of plain cylinders {**10**} have led to theoretical models for computing expansion and bursting strengths, based on tension and torsion data. For various steels, it has been shown that heat treatment has no effect on the OVP or bursting pressure {**11**}. Pressure combined with thermal treatment can produce a compressive residual stress in the inner and outer parts of tubes, applicable in the bend regions where stress corrosion cracking is a problem {**12**}. The most comprehensive theoretical study involved a stiffness method for the solution of elastic–plastic problems {**13**}. This concept enabled the equilibrium equations to be expressed in terms of displacements and removed the need to trace the expansion of the elastic–plastic boundary during the actual solution of the differential equations. This method was not suitable for perfectly plastic or very small degree of hardening materials. The plastic stress–strain matrix derivable by inverting the Pradtl–Reuss equations is used for the solution of continuum elastic–plastic problems using the finite element method (FEM) {**14**}. This method uses the small and varying increments of load sufficient to just cause yield in the successive elements and has greatly reduced the programming effort in the incremental theory of plasticity. Other FEM solutions to three-dimensional elastic–plastic problems, illustrating the applicability of the isoparametric elements and the order of computation times involved, have been presented {**15**}.

The effect of the yield stress and the strain hardening exponent of the material on the stress and strain levels has been studied in pipe bore expansion using the FEM. By considering that the effective stress and its approximation are given by {**16**}

$$\overline{\sigma} = Y_s + C\overline{\varepsilon^n} \tag{1}$$

$$\overline{\sigma} \approx C\overline{\varepsilon^n} \tag{2}$$

the indeterminacy of the initial condition was eliminated. The FEM has also been used in metal-forming problems, where finite-size deformations introducing instability have been taken care of by modifying the stiffness formulation by means of the mean normal technique {**17**}. The von Mises and Tresca yield theories have been compared in conditions of compressibility and incompressibility for elastic–plastic analysis of cylinders {**18**}. Large differences in stresses were observed from these two criteria. A closed-form theory to include the Hencky stress–strain relations, incompressibility and Ludwik strain hardening function was proposed. However, the work does not discuss which of the two criteria is more accurate.

Three-dimensional FEM analysis for plain cross-bored cylinders with a thickness ratio (k) of 1.4 and 2 and cross bore–main bore radius ratio (d) of 0.12 have been conducted {**19**} with few elements in the vicinity of the points of peak stresses and adjacent to the boundary being allowed to yield. Plastic strain components in the critical region of the cross bore were determined. The thickness ratio is defined as the ratio of the cylinder outer radius (R_o) to the inner radius (R_i). The author was mainly interested in fatigue life and no detailed data were provided. Three-dimensional analysis of cross-bored cylinders in partial autofrettage was carried out using the boundary integration method {**20**} for $k = 2$ and 2.25 and $d = 0.25$. Autofrettage was performed after the introduction of the cross bore. The maximum OVR induced was found to be 35 and 27.5 per cent for $k = 2$ and 2.25 respectively. The work did not cover enough cylinder bore–cross bore configurations and no conclusive results were obtained. An optimum OVR diameter has been proposed {**21**} as being equal to $2(R_i R_o)^{1/2}$ for medium-strength steels and slightly less for high-strength steels.

Approximate equations suitable for a numerical solution of an axisymmetric shell under axisymmetric loadings have been developed {**22**}. An incremental approach under consideration of the first-order approximation in determining the tangent stiffness characteristics of the finite element was used. The effects of isotropic and kinematic strain hardening were included. Initial stresses were given to account for instability and large accumulated deformations during the loading of the structure.

Autofrettage has been found to be useful in increasing the fatigue life of high-pressure piping, compressor chambers and similar thick-walled components {**23**}. Determination of residual stresses arising from forming, cold working or overstrain procedures is important, particularly where cross bores may exist. For monoblock plain cylinders under partial autofrettage, the analytical residual stresses may be obtained directly by applying an equivalent thermal load {**24**}. Simple destructive methods based on fracture mechanics have been developed for measuring residual stresses {**25**}, though they are not satisfactory for measuring the residual stress distributions where stress gradients are high. Sequential and selective destructive procedures employing incremental strain gauge data in the FEM algorithm to construct the initial residual stress distribution are currently in use {**26**}. Tensile residual hoop stresses are introduced in seamless gas cylinder necks at the bore during the heat treatment stage. At the neck, the outer surface experiences compressive hoop stresses and the bore experiences tensile hoop stresses. Material removal corrective procedures to remove the bore residual stresses have been established {**27**}. As a means of measuring autofrettage in thick-walled cylinders, an experimental method based on measuring the hoop strain while axisymmetrically releasing the residual stress field by introduction of radial cuts in the cylinder has also been proposed {**28**}. This is due to the fact that access to the cylinder inside surface for purposes of placing strain gauges is usually denied.

Closed-form solutions of residual stresses in autofrettaged steel tubes are available {**29**}. Models neglecting both strain hardening and Bauschinger effects overestimate the bore residual hoop stress by 46 per cent, while models including the Bauschinger effect only underestimate this value by 25 per cent. Analytical residual stresses for hardening and non-hardening materials considering the Tresca and von Mises yield criteria have been obtained {**30**} by using closed- and open-ended cylinders. The optimum OVR to prevent reverse yielding has been proposed and the overstrain has been found to prevent a reduction in fatigue life for cylinders with $k > 2.96$. The Tresca yield criterion results were admissible for $k < 2$ but the von Mises citerion was found to more practical for $k > 2$. The influence of strain hardening on open cylinders is important when $k \geqslant 3$. Linear elastic solutions can be used as a basis to generate an inelastic solution, which may then be used to predict the residual stress fields {**31**}. The dependency of the Bauschinger effect on plastic strains makes significant changes to residual hoop stress near the bore for low-level autofrettage, but this dependency was found to be insignificant for high-level autofrettage.

The evaluation of residual stresses inside the material or in very small cross bores is difficult without a destructive procedure. Though a lot of work has been dedicated to the evaluation of residual stresses in cylinders, no meaningful or broad study has been done in the presence of cross bores. A numerical method such as the FEM is suitable since no destructive procedures are involved and the state of residual stress at any location can be determined. The knowledge of the stress levels and distributions is important.

3 PROCEDURE

Due to inaccessibility of commercial software, a FEM computer program in FORTRAN code was developed to carry out the elastic–plastic analysis {**5**, **32**} of the plain cross-bored cylinder. An internal pressure was simulated to act on both the main and cross bore surfaces. The cylinder was closed ended. An elastic module of the program has been successfully used to perform an elastic analysis of the same structure {**33**}. The quarter cylinder geometry for the structure is shown in Fig. 1. The applicable boundary conditions are that the nodes in the y–z plane have no displacement in the x direction and the nodes in the x–z plane have no displacement in the y direction. The displacement formulation was adopted when the eight-noded isoparametric element (see Fig. 2) having eight Gauss points was used.

The overall geometrical inputs were the outer radius, inner radius (75 mm), length of cylinder (nine times the thickness) and radius of the cross bore (see Fig. 1). The number of elements was input for lines CD (14), CI (12), HG (3), AB (6) and CB (6). The nodal spacing geometric ratios on lines CB (1.5), CD (1.5), HG (5) and AB (0.95) were also input. The geometric ratios for the nodal spacing along the respective edges ensured that in the region with high stress gradients the element sizes were very small, in conformity with the FEM procedures. Also input was the length of line HI (10 per cent of the main bore radius). This resulted in a structure with 2580 nodes, 2016 elements, 7740 degrees of freedom and a frontal width of 801. The global stiffness matrix coefficients for memory storage were reduced by 99 per cent; $k = 1.25$–3 and $d = 0.005$–0.4 were used. The above data completely defined the geometry. The geometric ratios were used in controlling the element

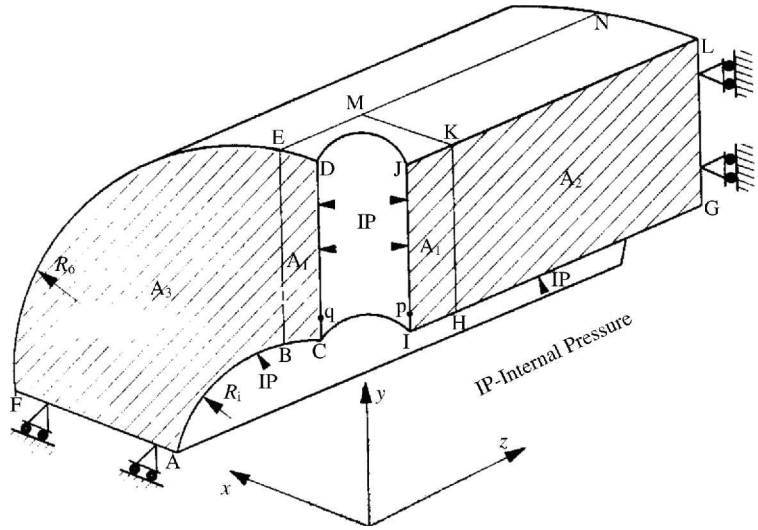

Fig. 1 Discretization of a plain cross-bored cylinder

aspect and volume ratios and were also employed where high-stress gradients were anticipated.

The choice of the number of elements and geometric ratios in each division or line edge was based on the following: for parts away from the cross bore, to ensure that the far-field stresses were close to the exact solution of a plain cylinder; in the cross bore areas, to ensure that the SCF reasonably converged while minimizing the frontal width and processing time {**5**}. The stress concentration factor (SCF) is defined as the ratio of the maximum hoop stress around the cross bore region to the far-field hoop stress. The pressure vessel material was a high-strength SA-372 steel having a yield stress of $450\,\mathrm{N/mm^2}$, a Poisson ratio of 0.29 and a Young modulus of $209 \times 10^3\,\mathrm{N/mm^2}$ {**34**}. To obtain the displacements, Gauss point strains and stresses, the frontal solution technique {**35**} was employed. In the elastic–plastic range, the incremental theory of plasticity and the plastic stress–strain constitutive matrix were used {**14**}. Stress projection followed by tensor transformation techniques {**36**} were employed to obtain cylindrical coordinate stress curves for the nodal arrays.

An elastic perfectly plastic material obeying the von Mises yield criterion was assumed. The Bauschinger effect was not included since reverse yielding was not allowed. During the overstrain process, any element that attained an effective stress which was within 5 per cent of the material yield stress was considered to have yielded {**14**}. Whereas this procedure has the effect of introducing errors, it reduces the number of loading cycles necessary before a given OVR is achieved. A more stringent yield condition of 0.5 per cent was also demonstrated in order to assess the degree of error associated with the 5 per cent yield condition. Various OVR values were considered.

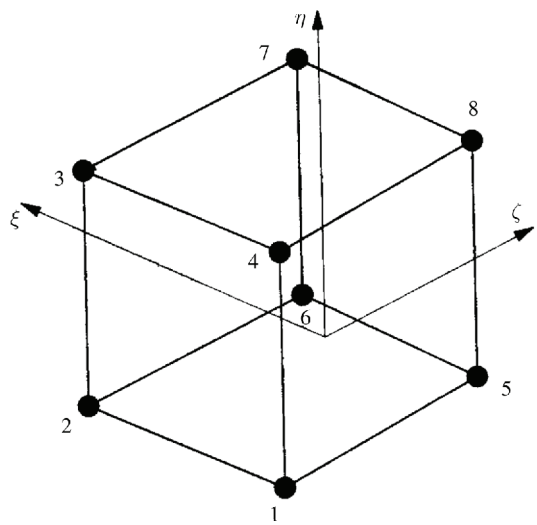

Fig. 2 Isoparametric eight-noded brick element

4 RESULTS AND DISCUSSION

4.1 Overstrain stresses

For clarity, the stresses and OVP results are shown as the stress–yield stress ratio (σ/Y_s) and the OVP–yield stress ratio (OVP/Y_s) respectively. The overstrain stresses are the stresses that occur when a cylinder is under OVP. The stresses presented in this section refer to the global hoop, radial, axial and effective stresses in the cylindrical coordinate system of the cylinder and are not referred to the cross bore local coordinate system. The overstrain hoop stresses for nodes on the cross bore surface are shown in Fig. 3 for OVR = 7 per cent, $k = 2.25$, $d = 0.1$ and an internal pressure ratio of 0.21. The location of the node in the meridional plane is shown as a ratio of its distance from the crotch corner to

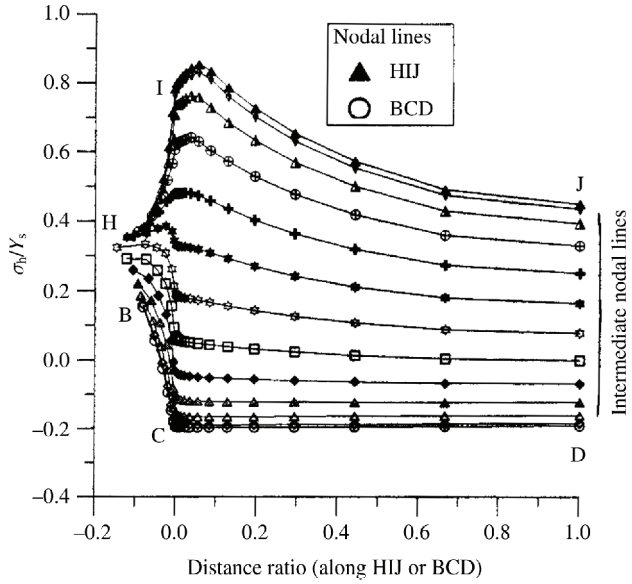

Fig. 3 Hoop stresses around a cross bore for OVR = 7 per cent ($k = 2.25$, $d = 0.1$)

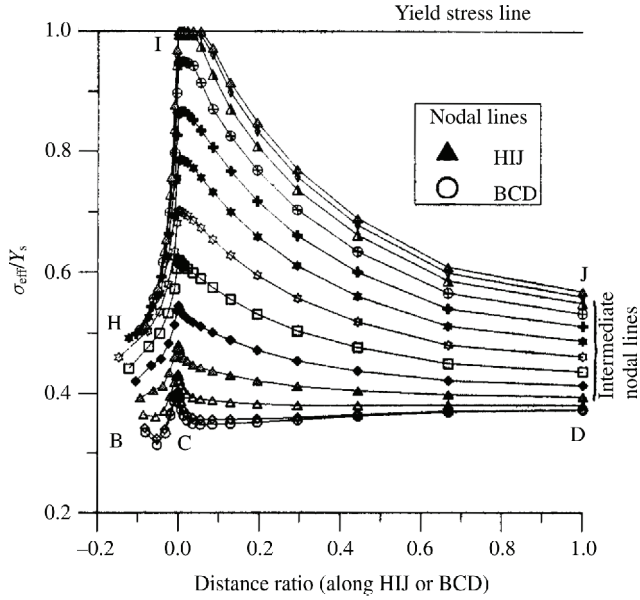

Fig. 4 Effective stresses around a cross bore for OVR = 7 per cent ($k = 2.25$, $d = 0.1$)

the cylinder wall thickness, measured in the direction approaching the cylinder outer surface. For clarity, only the nodes in the meridional plane (HIJ) and transverse plane (BCD) are shown in the legend. The remaining stress curves represent the nodes in the intermediate planes. The meridional plane (y–z plane) has been shown to be the critical plane in loaded plain cross-bored cylinders {**5**, **32**, **33**} and therefore the results presented mainly address the stresses in this plane.

The stress patterns are similar to those of an elastic analysis of the same configuration {**5**}. The levels are higher both for positive and negative stresses since the pressure is higher than that used in elastic analysis. Figure 4 shows the overstrain effective stresses for the same nodes. The effective stresses are higher and nodes within 15° of the crotch corner in the x–z plane have already yielded. The stress curves are very close around point I, indicating that the elastic–plastic front is rather narrow in the x–z plane and does not spread out much along the IC direction.

The overstrain stresses along the meridional curve HIJ are shown in Fig. 5 for OVR = 7 per cent. The radial stress ratio has a value of about −0.22 at point H. At the crotch corner, it reduces asymptotically, approaching zero along line IJ. This behaviour is normal since radial stresses are expected to vanish at point J. The axial stress ratio has a value of about 0.05 at point H and drops to about −0.17 at point I, remaining at this level along line IJ. The hoop stress ratio has a value of 0.39 at point H and rises sharply to reach a value of 0.84 at a point between points I and J. This is followed by a gradual drop. It is notable that the location of the maximum hoop stress has now moved deeper inside the wall thickness, coinciding with the elastic–plastic interface. The elements already yielded tend to have a lower hoop stress. This behaviour is normal in plain cylinders {**5**} where the outer elastic shell tends to restrain the inner plastic core from moving out in the radial direction, thus reducing the hoop stress. The crotch corner plus the adjacent elements along IJ have yielded while the rest on either side of point I are still elastic. The elastic–plastic behaviour around the cross bore is not quite like that of the plain cylinder {**5**}. In this case, the elastic shell is not perfect since some elements are on the free cross bore surface and are not

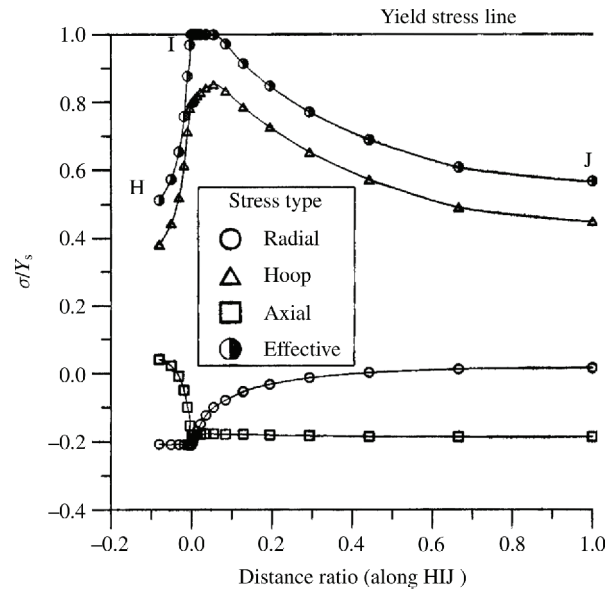

Fig. 5 Meridional stresses for OVR = 7 per cent ($k = 2.25$, $d = 0.1$)

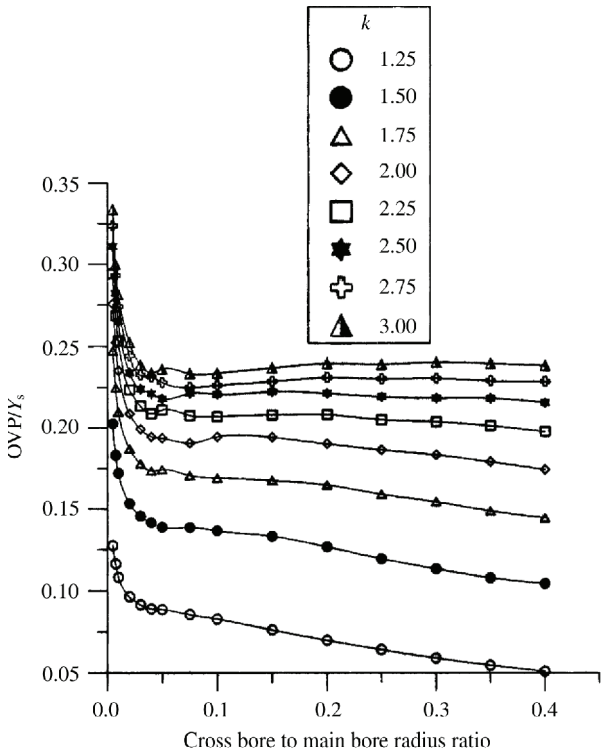

Fig. 6 Internal pressure versus d for OVR = 0.3 per cent

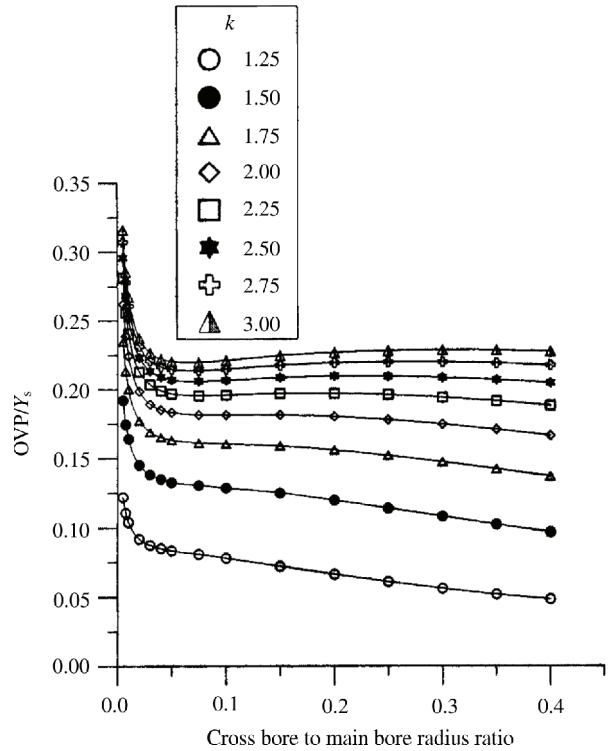

Fig. 7 Incipient yield pressure versus d

restricted to the same boundary conditions as those in the plain cylinder case. The yielding of an element on the cross bore surface weakens that particular point, causing a redistribution in the local structural stiffness. The local displacements and stresses are therefore not as predictable as those in a plain cylinder.

The OVP to achieve an OVR of 0.3 per cent for $k = 1.25$–3 and $d = 0.005$–0.4 are shown in Fig. 6. For a given d, the pressure increases with increasing k. For each k, the maximum pressure is observed for the lowest d. As d increases, the pressure drops sharply, with the gradient increasing as k increases. The 0.3 per cent OVR means a higher absolute dimension in the higher than in the lower k cylinders and therefore more pressure is required for the same OVR level. The variation of the incipient yield pressure with respect to d is shown in Fig. 7. The incipient pressure patterns are similar to those in Fig. 6. The curves are smooth since only one element is loaded to the yield point during the incipient yield process and the structural stiffness adjustments associated with the OVP have not taken place. The figures provide quick look-up tables in the process of autofrettage and help to select the correct OVP for the desired configuration.

To understand the cylinder response to increasing OVR, the cylinder was subjected to OVR = 7–83 per cent. The meridional overstrain hoop stresses are shown in Fig. 8. For each OVR, the maximum stress occurs at

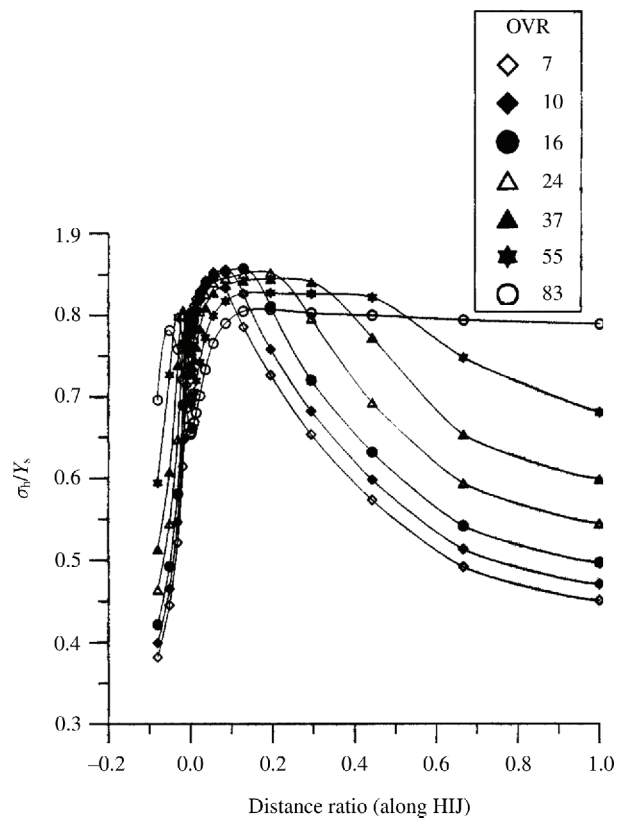

Fig. 8 Meridional hoop stresses for varying OVRs ($k = 2.25$, $d = 0.1$)

the elastic–plastic interface and progressively decreases in magnitude and shifts away from the crotch corner in the radial direction as the OVR is increased. The stresses increase very rapidly along line HI. At the crotch corner, the stress drops sharply and then rises along line IJ. The extent of this rise is governed by the elastic–plastic interface location. The decrease is highest for OVR = 83 per cent. This decrease is due to the stress redistribution, which arises from yielded elements having a lowered stiffness. Each of the curves has a plateau once the maximum stress is achieved and before the interface. Figure 9 shows the meridional overstrain effective stresses and clarifies how the elastic–plastic interface location shifts with an increase of the OVR. At OVR = 83 per cent, all the nodes along line IJ have yielded. This through-thickness yielding should always be avoided since there is no elastic shell containment in the global coordinate system to hold the material from deforming to limits outside the cylinder outer shell. This situation could lead to gross deformation and rupture of the cylinder at the cylinder edge around point J. However, in the cross bore local coordinate system, the elastic containment may be considered to exist, though it is not uniformly distributed about the full arc of the cross bore. This non-uniformity introduces further complexity in the overstrain stress system around the cross bore. The variation of the OVR with the OVP is shown in Fig. 10. For OVR $\leqslant$ 7 per cent, the OVP is constant for the 5 per cent yield condition. The more stringent yield condition of 0.5 per cent shows a straight curve for these low OVR values.

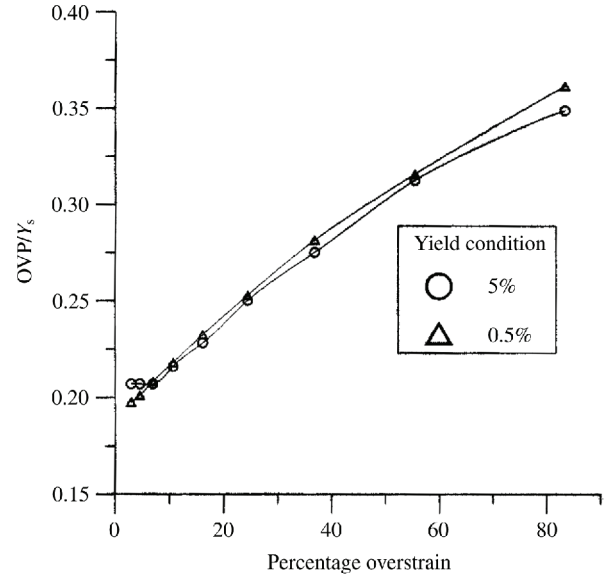

Fig. 10 Pressure versus OVR for two yield conditions ($k = 2.25, d = 0.1$)

4.2 Residual stresses

The meridional residual hoop stresses are shown in Fig. 11 for varying the OVR and for $k = 2.25$ and $d = 0.1$. For nodes along line HI, the stress drops sharply, reaches a minimum value and then rises asymptotically, approaching zero away from the crotch corner. The nominal minimum value increases with an increase in the OVR. The 83 per cent OVR curve shows a minimum stress ratio of about -0.8. After the drop in stress, the point at which the curves attain a zero value is dependent on the OVR, this point progressively moving

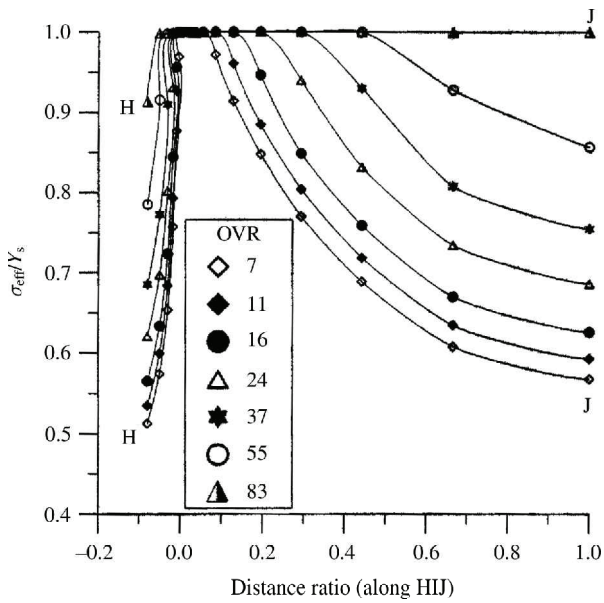

Fig. 9 Meridional effective stresses for varying OVR ($k = 2.25, d = 0.1$)

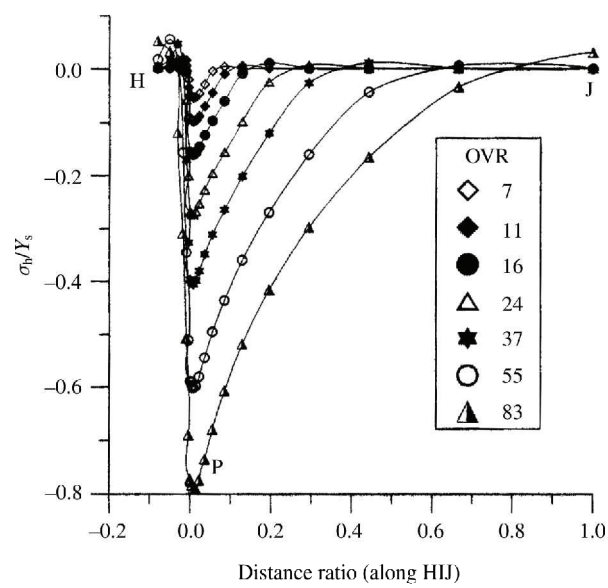

Fig. 11 Meridional residual hoop stresses for varying OVRs ($k = 2.25, d = 0.1$)

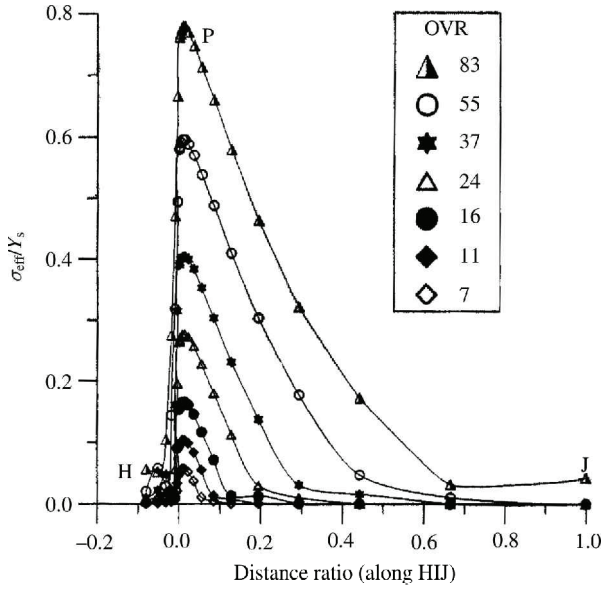

Fig. 12 Meridional residual effective stresses for varying OVRs ($k = 2.25, d = 0.1$)

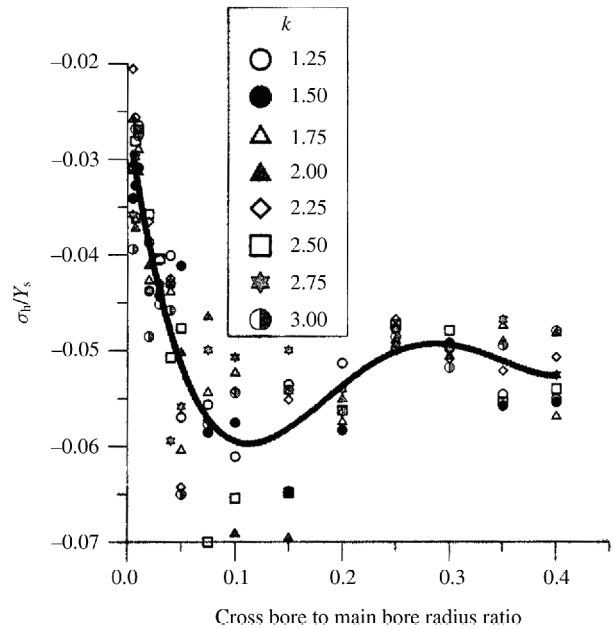

Fig. 13 Minimum residual hoop streses versus d for OVR = 7 per cent

away from the crotch corner as the OVR is increased. Figure 12 shows the corresponding effective stresses for the varying OVR. These curves are almost a mirror image of the hoop stresses about the line $y = 0$, as shown in Fig. 11. The curves show a maximum stress at a point away from and around the crotch corner. This maximum increases with an increase in the OVR. The 83 per cent OVR curve has a maximum stress ratio value of about 0.78. The higher the value of the hoop stress, the better the cylinder is predisposed to accommodate further positive pressure loading in service. However, the residual stress system should not be such that reverse yielding of the elements takes place. This would induce cycling in service, which may lead to early fatigue failure.

An interesting and yet to be fully explained observation is the variation of the minimum residual hoop stress with d, as shown in Fig. 13. The curves have no gradual variation but tend to have scattered and unpredictable points. However, as a group, the general variation is predictable and may be approximated using a polynomial curve (of fifth order). It is important to note that the maximum hoop stress for the elastic {**5**} and elastic–plastic curves do not lie at the same point as d changes. The elastic–plastic interface shape and extent varies from one d to the other. This has the effect of changing the resultant superposed residual stress system in a rather unpredictable manner. This behaviour could be further confirmed by adopting the more stringent yield condition. The variation of the minimum residual hoop stress for varying the OVR is shown in Fig. 14 for $k = 2.25$ and $d = 0.1$. The curve shows an increase in the nominal value of the minimum stress with an increasing OVR and is similar to Fig. 10. Different yield conditions are considered.

The method of overstraining in this work is such that a cylinder with a plain cross bore is overstrained to the desired level and then offloaded with a negative pressure equal to the OVP. This means that the full effects of autofrettage are only felt by the elements around the cross bore. This process does not achieve the true benefits of autofrettage and is limited in order to avoid through-thickness yielding of the elements. For the

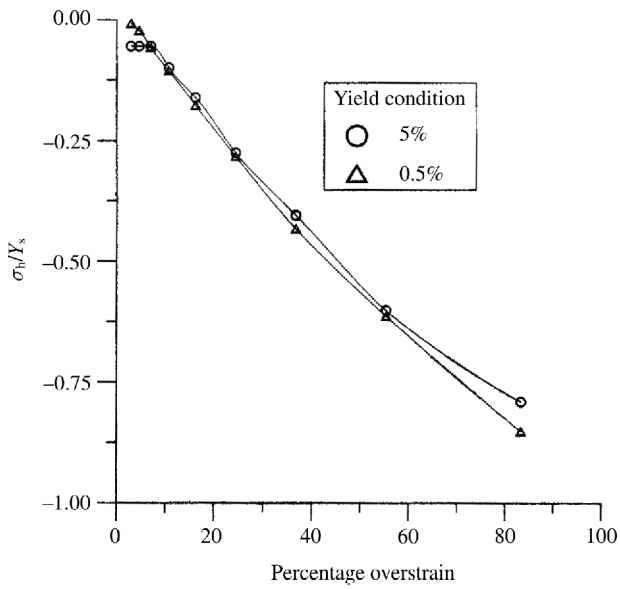

Fig. 14 Minimum residual hoop stress for two yield conditions

whole cylinder to experience autofrettage, it would be necessary that a plain cylinder is first autofrettaged to the required OVR. The cross bore should then be introduced and overstrained. The resultant residual stress system around the cross bore for that set-up would be interesting to compare with the results in this work. A future research work will address this approach of achieving overstrain.

4.3 Service stresses

In assessing the benefits of autofrettage, it is important to quantify and demonstrate the service stress levels and their distributions around the cross bore. For $k = 2.25$ and $d = 0.1$, the in-service meridional hoop stresses are shown in Fig. 15 for a selected number of OVR values and an internal pressure ratio of 0.09. For 0 per cent OVR, the maximum stress occurs at point P away from the crotch corner [5]. Increasing the OVR results in lower minimum stresses accompanied by a decreasing maximum. As the OVR is increased, point P does not become the point of minimum stress. The point having a minimum stress is located between point P and the crotch corner. Towards points J and H, the stresses have the same value for all OVRs. Between points I and P, the stress has very high gradients. This is in contrast to the 0 per cent OVR case. The 37 per cent OVR case results in the minimum stress and this has a negative value. Negative service hoop stresses have the advantage of stopping any crack-like flaws, especially near the crotch corner from propagating. It can be deduced that the cylinder can now accommodate much higher pressures before re-yielding can take place. This can be useful in preventing accidental overpressure damage in the case of short-term overpressure control failure. A negative residual hoop stress should be accompanied by a negative service hoop stress if stress reversals are to be avoided. In terms of hoop stress, the new distribution is not as smooth as that of 0 per cent OVR. The corresponding effective service stresses are shown in Fig. 16, where the point of minimum effective stress coincides with the point of minimum hoop stress. For OVR >16 per cent the maximum effective stress occurs between points H and I. This also applies to the hoop stresses.

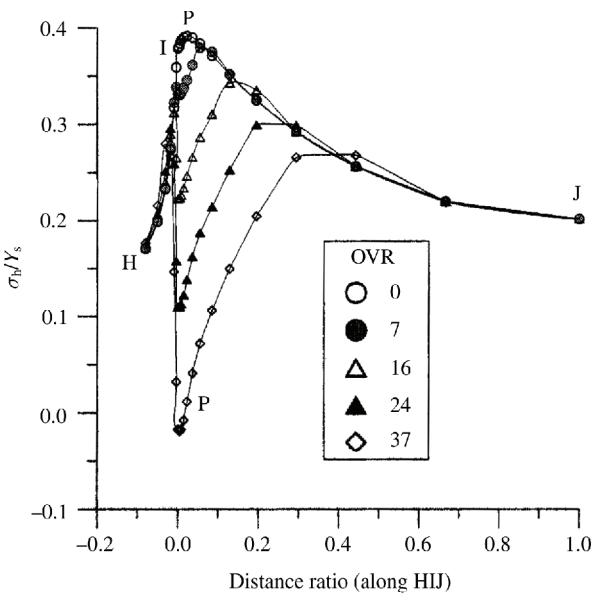

Fig. 15 Service hoop stresses for varying OVRs ($k = 2.25, d = 0.1$)

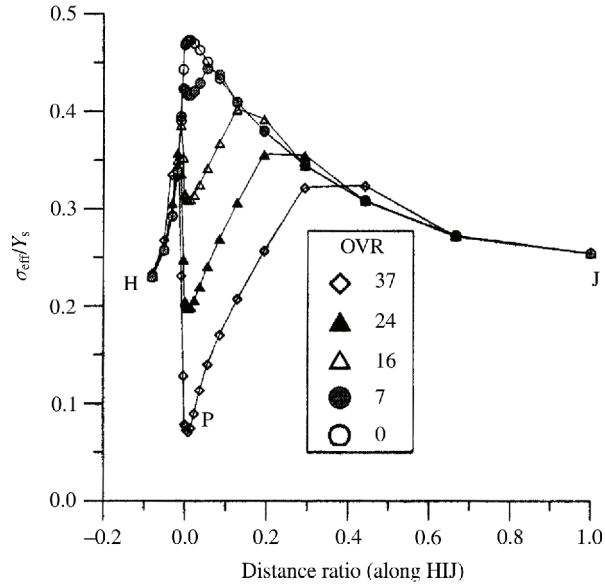

Fig. 16 Service effective stresses for varying OVRs ($k = 2.25, d = 0.1$)

5 CONCLUSIONS AND RECOMMENDATIONS

The incipient yield pressures were established for varying k and d. The collected data could be a reliable guide when elastic–plastic conditions are to be avoided for elastic service. For OVR $= 0.3$ per cent, the OVPs were established for varying k and d. For $k = 2.25$, $d = 0.1$ and varying OVR, the overstrain, residual and service stress levels and profiles have been presented and the resultant stresses discussed. The overstrain process was found to result in favourable residual and service stress systems, especially beyond an OVR of 37 per cent when the service hoop stress was negative and the operating pressure ratio could not go beyond the value of 0.21. An operating pressure beyond this value would cause stress reversals at some points, leading to possibility of fatigue failure. At 7 per cent OVR, all the elements within 30° of the transverse plane and near

the cross bore had negative hoop stresses for $k = 2.25$ and $d = 0.1$.

In using any of the yield conditions, some error was retained through the method of averaging the Gauss point stresses to determine whether an element has yielded. In reality, some Gauss points within an element yield while others are still elastic. This was observed in the high stress gradient regions. However, this error could be reduced by further refinement of the elements around such geometrical points. Another and more economical approach would be to alter the yield condition in such a way that the nodes rather than the elements would be allowed to yield for the yield condition to be satisfied.

REFERENCES

1 **Zapfec, C. A.** Boiler embrittlement. *Trans. ASME*, 1942, **66**(2), 81–126.
2 **Bush, S. H.** Statistics of pressure vessel and piping failures. *J. Pressure Vessel Technol.*, August 1988, **110**, 225–233.
3 **Iwadate, T.**, *et al.* Safety analysis at a cross bore corner of high pressure polyethylene reactors. In International Conference on *Pressure Vessels and Piping: Materials, Nuclear Engineering and Solar Energy; Trans. ASME*, 1981, **103**.
4 **Masu, L. M.** The effect of cross bore geometry on the strength of pressure vessels. PhD thesis, University of Leeds, 1989.
5 **Kihiu, J. M.** Numerical stress characterization in cross-bored thick walled cylinders under internal pressure. PhD thesis, University of Nairobi, 2002.
6 **Faupel, J. H.** and **Harris, B.** Stress concentrations in heavy walled cylindrical pressure vessels. *J. Ind. Engng Chemistry*, 1957, **49**.
7 **Faupel, J. H.** Yield and bursting characteristics of heavy-wall cylinders. *Trans. ASME*, July 1956, **78**(5).
8 **Davies, L. M., Garne, L.** and **Collier, J. G.** Second Marshall Study Group on PWR pressure vessel integrity. *J. Pressure Vessel Technol.*, February 1983, **105**, 53–57.
9 **Ford, H.**, *et al.* Thoughts on a code of practice for forged high pressure vessels of monobloc design. *Trans. ASME*, 1981, **103**.
10 **Jorgensen, S. M.** Overstrain tests on thick walled cylinders. *J. Engng for Industry*, 1960, 103–121.
11 **Faupel, J. H.** and **Furbeck, A. R.** Influence of residual stresses on behaviour of thick walled closed-end cylinders. In 7th National Instruments Conference, Cleveland, Ohio, 9–10 September 1952.
12 **Le, N. V.** Method and mechanism of beneficial residual stresses in tubes. *J. Pressure Vessel Technol.*, May 1994, **116**, 175–178.
13 **Marcal, P. V.** A stiffness method for elastic plastic problems. *Int. J. Mech. Sci.*, 1965, **7**, 220–238.
14 **Yamada, Y.**, *et al.* Plastic stress strain matrix and its application for the solution of elastic plastic problems by the finite element method. *Int. J. Mech. Sci.*, 1968, **10**, 343–354.
15 **Owen, D. R. J.** and **Salonen, E. M.** Three dimensional elastic plastic finite element analysis. *Int. J. Numer. Meth. Engng*, 1975, **9**, 209–218.
16 **Tomita, Y.**, *et al.* Axisymmetric deformation of circular elastic plastic tubes under axial tension and internal pressure. *Int. J. Mech. Sci.*, 1984, **26**(6–8), 437–444.
17 **Pillinger, I.**, *et al.* Use of mean normal technique for efficient and numerically stable large strain elastic plastic finite element solutions. *Int. J. Mech. Sci.*, 1986, **28**(1), 23–29.
18 **Steele, M. C.** Partially plastic thick-walled cylinder theory. *J. Appl. Mechanics*, June 1952, **19**, 133–140.
19 **Masu, L. M.** Plasticity analysis and cross bore size effects on the fatigue strength of thick walled cylinders. *E. Afr. J. Engng*, 1994, **1**(2), 22–23.
20 **Tan, C. L.** Stress distributions in thick walled cylinders due to the introduction of bore after autofrettage. *J. Strain Analysis*, 1986, **21**.
21 **Jorgensen, S. M.** Overstrain and bursting strength of thick-walled cylinders. *Trans. ASME*, April 1958, **80**(3), 561–570.
22 **Dudans, Z.** Finite element incremental elastic–plastic analysis in pressure vessels. *J. Engng for Industry*, May 1970, 293–302.
23 **Hsu, L. C.** Analysis for design—Part 1: introduction. In *Pressure Vessels and Piping: Design and Analysis*, Vol. 1, *Analysis*, 1972.
24 **Hussain, M. A.**, *et al.* Simulation of partial autofrettage by thermal loads. *J. Pressure Vessel Technol.*, August 1980, **102**, 314–318.
25 **Zhou, H.** and **Rao, M. D.** On the error analysis of residual stress measurements by the hole drilling method. *J. Strain Analysis*, 1993, **28**(4), 273–276.
26 **Sharman, D. J.**, *et al.* Bench marking of a destructive technique to determine residual stresses in thick walled axisymmetric components. *J. Strain Analysis*, 1997, **32**(2), 87–96.
27 **Sharman, D. J.**, *et al.* A comparison of potential methods for the alleviation of residual stresses in the necks of aluminium alloy thick-walled gas cylinders. *J. Strain Analysis*, April 1997, **32**(5), 315–323.
28 **Perl, M.** and **Arone, R.** An axisymmetric stress release method for measuring the autofrettage level in thick-walled cylinders—Part I: basic concept and numerical simulation. *J. Pressure Vessel Technol.*, November 1994, **116**, 384–388.
29 **Chen, P. C. T.** The Bauschinger and hardening effects on residual stresses in an autofrettaged thick walled cylinder. *J. Pressure Vessel Technol.*, 1986, **108**, 109–112.
30 **Rees, D. W. A.** Autofrettage theory and fatigue life of open ended cylinders. *J. Strain Analysis*, 1990, **25**(2), 109–121.
31 **Jahed, H.** and **Dubey, R. N.** An axisymmetric method of elastic–plastic analysis capable of predicting residual stress field. *J. Pressure Vessel Technol.*, August 1997, **119**, 264–273.
32 **Kihiu, J. M., Mutuli, S. M.** and **Rading, G. O.** Stress characterization in autofrettaged thick walled cylinders. *Int. J. Mech. Engng Educ.*, 2003, **31**(4), 370–389.
33 **Kihiu, J. M., Rading, G. O.** and **Mutuli, S. M.** Geometric constants in plain cross-bored cylinders. *J. Pressure Vessel Technol.*, 2003, **125**, 446–453.

34 Mraz, G. J. and **Nisbett, E. G.** Design, manufacture and safety aspects of forged vessels for high pressure service. *J. Pressure Vessel Technol.*, 1980, **102**, 99–106.

35 Irons, B. M. A frontal solution program. *Int. J. Numer. Meth. Engng*, 1970, **2**, 5–32.

36 Hinton, E. and **Campbell, J. S.** Local and global smoothing of discontinuous finite element function using a least square method. *Int. J. Numer. Meth. Engng*, 1974, **8**, 461–480.